Hindawi
Journal of Nanomaterials
Volume 2017, Article ID 2758294, 13 pages
https://doi.org/10.1155/2017/2758294

Research Article

Preparations, Characterizations, and a Comparative Study on Photovoltaic Performance of Two Different Types of Graphene/TiO_2 Nanocomposites Photoelectrodes

Uea-aree Kanta,[1] Voranuch Thongpool,[2] Weradesh Sangkhun,[1] Nutthapon Wongyao,[3] and Jatuphorn Wootthikanokkhan[1]

[1]*Nanotec-KMUTT Center of Excellence on Hybrid Nanomaterials for Alternative Energy (HyNAE), School of Energy, Environment and Materials, King Mongkut's University of Technology Thonburi, Bangkok 10140, Thailand*
[2]*Division of Physics, Faculty of Science and Technology, Rajamangala University of Technology Thanyaburi, Klong 6, Thanyaburi, Pathum Thani 12110, Thailand*
[3]*Fuel Cells and Hydrogen Research and Engineering Center, King Mongkut's University of Technology Thonburi, Bangkok 10140, Thailand*

Correspondence should be addressed to Jatuphorn Wootthikanokkhan; jatuphorn.woo@kmutt.ac.th

Received 5 September 2016; Revised 15 December 2016; Accepted 10 January 2017; Published 21 March 2017

Academic Editor: Xuping Sun

This research work undertook a comparative study of the promoting effects of graphene in TiO_2 photoanodes. The aim of this work was to investigate the effects of the types and concentration of reduced graphene oxides (rGO) on structure properties and the photovoltaic performance of TiO_2 based electrodes. Graphene oxide (GO) was prepared by using modified Hammer's method. Next, GO was reduced by using two different approaches, which were the chemical reduction with vitamin C and thermal reduction. The latter approach was also carried out in situ during the fabrication and heat treatment processes of the dye-sensitized solar cells (DSSCs). From the results, it was found that the photovoltaic performance of the DSSCs containing the GO/TiO_2 electrode, in which the GO phase experienced an in situ thermal reduction, was superior to those containing rGO/TiO_2. It was also found that the power conversion efficiency of the DSSCs changed with the concentration of graphene in a nonlinear fashion. The optimum concentrations of graphene, corresponding to the highest PCE values of the GO/TiO_2 based DSSC (3.69%) and that of the rGO/TiO_2 based cell (2.90%), were 0.01 wt% and 0.03 wt%, respectively.

1. Introduction

The development of materials for the new generation of solar cells has been an interesting subject that has gained more and more interest over the past decade. This is attributed to several advantages of immerging photovoltaic devices, including the relatively low cost and simple fabrication process and the possibility of enlarging the production scale by using existing industrial technologies, such as printing. Besides, the photovoltaic performance of this new generation of solar cells is also interesting. At the present time, the power conversion efficiency values of the best research organic photovoltaic cell (OPV), dye-sensitized solar cell (DSSC), and the perovskite solar cell (PSC), certified by the NREL, are 11.5%, 11.9%, and 22.1%, respectively [1]. However, further developments have yet to be carried out before these devices can be mass-produced and used commercially. These include three main research issues which are (1) the improvement of stability and lifetime of the solar cell, (2) the development of alternative materials which are less toxic and of lower cost, and (3) the enhancement of their cell efficiency, taking into account the fact that the enlargement of the cell size and its active area is usually achieved at the expense of cell efficiency. To achieve the above goals, several approaches have been used, including the development of better materials and the designs of new solar cell configuration and architecture.

Nanocrystalline titanium dioxide film (TiO_2) coated on a transparent conductive oxide glass has been widely used

as a photoanode in many types of the new generation solar cells, including DSSC and PSC. In this context, the transportation of the photogenerated electrons across the TiO_2 nanoparticles network is considered to be one important factor determining the performance of the solar cell. Without efficient charge transport, electron-hole recombination can occur, and that can lead to a relatively low efficiency of the cells. To enhance the electron transport of a DSSC photoelectrode, TiO_2 might be treated with some chemicals such as nitrogen, Sn, Cu, Zr, CNT, and graphene. For example, Ding et al. [2] prepared reduced graphene oxide (rGO) by treating graphene oxide (GO) with a reducing agent prior to mixing with TiO_2 of various weight compositions (0.25–1.25 wt% of rGO). The rGO/TiO_2 composite was then applied as a photoanode for the DSSC and the photovoltaic performance was studied. It was found that the power conversion efficiency of the DSSC changed with the concentration of rGO in a nonlinear fashion. Specifically, the PCE values initially increased with the concentration of rGO to the maximum and then decreased again with a further increase of rGO. The greatest PCE value (7.89%) was obtained when 0.75 wt% of rGO was added to the TiO_2. Alternatively, Tang et al. [3] incorporated rGO into TiO_2 via molecular grafting. In that experiment, by properly controlling the oxidation time during the chemical exfoliation process, the hydroxyl groups on the surface of the graphene sheet were optimized, and a strong interaction between rGO and TiO_2 was induced, through the chemisorption. As a result, the PCE values of the DSSCs increased by more than five times compared to that of the cell containing the bare TiO_2 electrode. Recently, a rGO/TiO_2 electrode was also applied to a perovskite solar cell (PSC). For example, work by Han et al. [4] demonstrated that the solar cell based on rGO/TiO_2 nanocomposite electrode had higher J_{sc}, fill factor, and V_{oc} values than those of the devices based on the bare TiO_2 electrode. By properly controlling the film thickness and dispersion of rGO, the maximum PCE value of the PSC (14.5%) was obtained when 0.4 vol% of rGO was added to the TiO_2. This accounted for approximately an 18% increase, as compared to that of the normal PSC based on a bare TiO_2 electrode (11.5%).

Practically, graphene, in a form of colloidal suspension, can be prepared via exfoliation of graphene oxide (GO) followed by a chemical reduction. Reducing agents that can be used for the chemical reduction of GO include hydrazine, dimethyl hydrazine, hydroquinone, and $NaBH_4$ [5]. Particularly, hydrazine is widely used for reduction of GO because of its high efficiency as compared to that of other chemicals. However, the obtained graphene is unstable in water. It can be aggregated owing to the strong van der Waals force between molecules. To further enhance stability and dispersion of graphene in aqueous media, Swain and Bahadur [6] added two cross-linking polymers, polyvinylpyrrolidone (PVP) and poly(vinyl alcohol) (PVA), to the hydrazine based reduction process. However, most of the abovementioned reducing agents are known to be toxic and some of them can be explosive. In this regard, attempts have been made to explore the use of some alternative reducing agents to prepare graphene. For example, Fernández-Merino et al. [7] and Zhang et al. [8] reported the use of L-ascorbic acid (vitamin C) as a reducing agent for preparing GO at room temperature. The results claimed that the average electrical conductivity values of the rGO prepared by vitamin C are comparable to those obtained by using hydrazine.

Alternatively, GO can be reduced via other processes such as photoreduction [9, 10], electrochemical reduction [11], and thermal treatment at temperatures ranging between 100 and 150°C [12]. In this study, a reduction of GO via the thermal treatment is of interest because this approach could be suitable with the DSSC application, taking into account the fact that the TiO_2 coated FTO usually underwent heat treatment (or annealing) during the fabrication process in order to get rid of some organic residual. In relation to this study, it can be expected that the GO phase in the GO/TiO_2 composites could be in situ reduced during annealing. This means that the GO might be applied to the solar cell system without undertaking a prereduction step. In fact, better photovoltaic performance of the thermally reduced GO/TiO_2 photoelectrode has been demonstrated by several researchers. For example, Wang et al. [13] found that the optimum content of GO was 0.83 wt%. This contributes to the increase in PCE of the DSSC from 1.79% to 2.78%. Kusumawati et al. [14] reported that the power conversion efficiency of the DSSC increased from 5.78% to 7.49% when 1.2 wt% of GO was added to the TiO_2 photoelectrode. Cheng and Stadler [15] modified TiO_2 with GO and found that the power conversion efficiency of DSSC containing 1.6 wt% of GO in the composite electrode (GO/TiO_2) was 7.68%, which is much greater than that which employed the bare TiO_2 electrode (4.78%). Chou et al. [16] reported that when about 1.5 mL of GO solution was mixed with TiO_2, the optimum PCE value (5.26%) of the DSSC containing the composite electrode was obtained.

From the above literature, it is evident that graphene is an effective and interesting chemical that can be used to modify TiO_2 to enhance the photovoltaic performance of the electrode in dye-sensitized solar cells. However, there has been no report on a comparative study of photovoltaic performance graphene/TiO_2 photoelectrodes, in which the reduced graphene oxide was prepared by using a different approach. It was believed that the optimum concentration of graphene for promoting TiO_2 was dependent on the systems and had yet to be optimized. In this study, the graphene/TiO_2 electrodes made from two different approaches were studied. These are (1) the system made by mixing GO with TiO_2 followed by an in situ thermal treatment (GO/TiO_2) and (2) the system prepared via prereduction of graphene oxide with vitamin C, followed by mixing it with titanium dioxide (rGO/TiO_2. More details concerning the preparation techniques can be found in the experimental part of this paper. The primary aim of this work is to investigate the effects of the type and concentration of graphene on structure properties and the photovoltaic performance of the TiO_2 based electrode. Attempts were also made to characterize the various materials and DSSCs, in terms of light absorption, percentage dye loading, and the interfacial electrical properties, in order to elucidate some possible mechanisms behind the promoting effect of graphene.

2. Experimental

2.1. Chemicals. Titanium dioxide (Evonik, P25, 75% anatase, average particle size of 21 nm), graphite (<20 μm, synthetic grade), isopropanol (99.5%, anhydrous), fluorine-doped tin oxide (FTO) glass (resistivity ~7 Ω/sq, with the thickness of glass and FTO of 2 mm and 660 nm, resp.), acetonitrile (99.8%, anhydrous), and *t*-butanol (99.5%, anhydrous) were purchased from Sigma-Aldrich. Sulfuric acid (95–97% AR grade), hydrochloric acid (37%, AR grade), and hydrazine (80% in water, synthesis grade) were obtained from Merck Co. Ltd. Dye (Ruthenizer 535-bisTBA, N719) was purchased from Solalonix and platinum paste was supplied from Solaronix. Potassium permanganate used was of AR grade from Ajax Finechem. Ascorbic acid (AR grade) was supplied by Suksapan Paint Co. Ltd. All of the above chemicals were used as received.

2.2. Synthesis of the Reduced Graphene Oxides. Graphene oxide (GO) was firstly prepared by using the modified Hummer method [17, 18]. Graphite powder (2.0 g) was mixed with 1.5 g of sodium nitrate and 46 mL of conc. sulfuric acid (H_2SO_4, 98%, aqueous) and stirred in an ice bath. Next, 6 g of potassium permanganate ($KMnO_4$) was gradually added, dropwise, to the content in the reaction flask at 20°C. The mixture was stirred for a further 3 h. Noteworthy is that the reaction between $KMnO_4$ and the graphite solution is exothermic and thus attempts were made to maintain the temperature below the ambient temperature (35°C). Next, 100 mL of deionized water was added to the mixture, followed by adding 10 mL of hydrogen peroxide (30% solution). During the addition of H_2O_2, change in color of the content in the reaction flask toward yellowish and eventually brown can be observed. This indicates that the residual permanganate and manganese dioxide were reduced [19]. After that, the product was washed with an aqueous solution of hydrochloric acid (2 M of 10% HCl) and the precipitate was further washed with deionized water until reaching neutral pH (pH = 7.0). Finally, the product was dried in an oven at 60°C until reaching a constant weight.

To reduce GO via a chemical treatment process, 0.3 g of the synthesized GO was dissolved in 100 mL of deionized water and then sonicated for 30 min. After that, 100 mg of ascorbic acid (vitamin C) was added to the solution and the mixture was sonicated for a further 2 h. The content in the reaction flask was filtrated and washed with distilled water several times to remove the remaining VC and residues. Finally, the filtrate was dried in an oven at 60°C for 12 h.

2.3. Preparation of Graphene Oxides/TiO_2 Composites (GO/TiO_2 and rGO/TiO_2). A given amount of the synthesized GO powder (varying from 0.2 to 0.6, 1.0, 2.0, and 3.0 mg) was dissolved in 100 mL of deionized water and sonicated for 30 min. Next, 2 g of a commercial nanocrystalline TiO_2 powder (P25, Degussa) was added to the GO dispersion and then sonicated for a further 1 h. The content in the reaction flask was filtrated and then washed with deionized water several times. Finally, the filtrate was dried in an oven at 60°C for 12 h. As a result, GO/TiO_2 nanocomposites with different concentrations of GO (0.01, 0.03, 0.05, 0.10, and 0.15 wt%) were prepared. In this study, the sample codes for the products were designated as TiO_2@GO-01, TiO_2@GO-03, TiO_2@GO-05, TiO_2@GO-10, and TiO_2@GO-15, respectively. For the preparation of reduced graphene oxide/TiO_2 nanocomposites, the synthesized rGO was used as a replacement of GO and similar steps were followed. In this case, the sample codes for TiO_2 electrodes containing different concentrations of rGO (0.01, 0.03, 0.05, 0.10, and 0.15 wt%) were designated as TiO_2@rGO-01, TiO_2@rGO-03, TiO_2@rGO-05, TiO_2@rGO-10, and TiO_2@rGO-15, respectively.

2.4. Preparation of the Electrodes. To prepare the TiO_2 based photoanode, fluorine-doped tin oxide (FTO) glass was cut into 25 × 25 (mm^2) square pieces. The FTO glass substrates were then treated with a hydrochloric acid solution (HCl, 0.2 M) in an ultrasonic bath for 15 min, followed by washing it with deionized water under the sonication process for 10 min, twice. After that, the substrates were cleaned with isopropyl alcohol and then dried by purging with nitrogen gas. In this study, to minimize some electron-hole recombinations at the interfacial zone between electrolyte and FTO layer, an electron transport layer (ETL) made from a thin film of TiO_x was applied into the cell configuration. The TiO_x sol-gel was firstly prepared by dissolving 0.1 M of titanium(IV) isopropoxide (TTIP) in isopropanol (IPA). Next, the TiO_x film coated onto the FTO glass was prepared by applying 10 μL of the TiO_x sol-gel onto the FTO glass substrate via a rapid convection deposition technique, at a deposition rate of 2 mm/s. The TiO_x coated FTO was then annealed at 500°C for 1 h. Next, different types of graphene oxides/TiO_2 nanocomposites were applied onto the ETL coated FTO glass. 10 μL of titanium tetraisopropoxide (TTIP) and 0.5 mL of ethanol were added to 0.20 g of the synthesized GO/TiO_2 (or rGO/TiO_2) powders, using a sonication process. The composite paste (GO/TiO_2 paste and/or rGO/TiO_2 paste) was then applied onto the ETL coated FTO glass by using a doctor blade technique. Specifically, a microscope slide (90° ground edges, Marienfeld Superior, from Paul Marienfeld GmbH & Co. KG, Germany) was used as a blade. The rGO/TiO_2 paste was placed and spread on the FTO substrate by manually moving the blade forward at the angle of 45° with respect to the FTO substrate. This process was repeated 8 times until a uniform thin sheet of the material was formed. Then, the prepared electrode was annealed at 450°C for 30 min, in order to get rid of some residual organic compounds originated from the graphene/TiO_2 paste and TiO_x precursor. At this stage, it is worth mentioning in the case of GO/TiO_2 electrode that it was expected that the GO phase in the composite layer would also be thermally reduced to graphene, leading to the formation of graphene/TiO_2 based photoelectrode. Finally, platinum coated FTO, used as a counter electrode, was prepared by coating Pt paste onto the FTO glass substrate via a doctor blade technique. The Pt coated FTO glass was then annealed at 500°C for 1 h.

2.5. Fabrication of the Dye-Sensitized Solar Cells (DSSCs). To commence the fabrication process of the DSSCs, the prepared photoanode had to be sensitized firstly by immersing it in

a staining jar, containing a solution of the dye (N719 in a cosolvent, 5 mL of anhydrous acetonitrile, and 5 mL of *tert*-butanol) at 80°C for 15 min. The staining jar was then kept in the dark for a further 18 h. After that, the dye absorbed photoanode was rinsed with anhydrous acetonitrile, followed by purging with nitrogen gas, and then dried in an oven at 80°C for 15 min. In this regard, the amount of dye loading in the photoelectrode was determined by using UV spectrophotometry, in combination with the Bear and Lambert equation, after complete dye desorption in a 0.1 mol·L^{-1} NaOH solution.

The prepared dye-sensitized photoanode was than assembled with Pt coated FTO counter electrode into a sandwich type cell, using a precut (4×3 cm^2 rectangular) sealing film (ethylene-acrylic acid copolymer, Surlyn from DuPont) as a frame. The cell was then sealed by applying a heat gun. Next, the electrolyte solution (HI-30 from Solaronix) was injected into the cells through a hole drilled in the counter electrode. Finally, the holes were plugged with the Kapton tape in order to avoid some leakage and evaporation of the liquid inside the cells.

2.6. Testing on Power Conversion Efficiency of the DSSCs. Current density-voltage (J-V) characteristics of the various cells were measured by using the Keithley 2400 source meter under 1.5 AM. The light source was generated by a solar simulator (Newport 91150 V model, 1000 W, xenon lamp), equipped with a 1.5 G air mass filter. The active area of the DSSC was 0.4×1.0 cm^2.

2.7. Characterizations. Functional groups in the chemical structures of synthesized graphene were monitored by using a Fourier transform infrared spectrometer (Thermo Nicolet 6700) in a transparent mode. The sample was prepared by using a KBr technique and the spectra were scanned over the wavenumber ranging between 500 and 4000 cm^{-1}. Reduction of GO was also followed up by a Raman technique, using the Raman spectrometer (NTEGRA Spectra, NT-MDT) equipped with a 532 nm laser.

Morphologies of graphene and graphene/TiO_2 composites were examined by using a scanning electron microscope (Nova NanoSEM 450, FEITM) equipped with secondary electron and EXD detectors. Crystal structures of the various materials including TiO_2, graphene based materials (GO, rGO), and the TiO_2/graphene composites were determined by using an X-ray diffraction (XRD) technique, using an X-ray diffractometer (PANalytical, X'Pert PRO) with Cu Kα radiation ($\lambda = 0.15406$ nm). The diffractometer was operated at 30 kV and 40 mA and the sample was scanned over a 2θ range of 0–80°. In addition, average crystal sizes of the TiO_2 phase in various composites were determined from XRD line-broadening of the TiO_2 (101) diffraction peals, using the Scherrer equation as follows:

$$D = \frac{K\lambda}{\Delta(2\theta)\cos\theta}, \quad (1)$$

where $\Delta(2\theta)$ is line-broadening at half the maximum intensity of the (101) peak of anatase, K is the coefficient (0.89), θ is the diffraction angle, and λ is the X-ray wavelength of Cu Kα radiation (0.15405 nm).

The reflectance spectra of TiO_2 and various graphene/TiO_2 composites, over the wavelength range between 200 and 800 nm, were measured using a UV-Vis-NIR spectrophotometer (Cary 5000, Agilent Technologies). From the reflectance value, the bandgap energy values of TiO_2 and graphene/TiO_2 composites were determined by using Kubelka-Munk's equation (2) and Planck's equation (3):

$$F(R) = \frac{(1-R)^2}{2R}, \quad (2)$$

where $F(R)$ is the Kubelka-Munk fraction and R is reflectance.

$$E_g = \frac{hC}{\lambda}, \quad (3)$$

where E_g is the bandgap energy (eV), h is Planck's constant (J/s), C is the speed of light (m/s), and λ is the cut-off wavelength (nm).

Electrochemical impedance analysis (EIS) of the various DSSCs was carried out in the dark at 0.75 V applied bias, using an impedance analyzer (Autolab-PGSTAT 302N). The impedance curves were recorded as Nyquist plots at 10 points per decade by superimposing 10 mV of AC signal onto the cell under potentiostatic mode with the frequency sweep from 1 MHz to 0.5 Hz.

3. Results and Discussion

3.1. Characterizations of the Synthesized Graphene. Figure 1 shows the FTIR spectra of graphite, graphene oxide, and the reduced graphene oxides. The absorption peak at 1635 cm^{-1} in the spectrum of the neat graphite, representing the carbon-carbon double bonds (C=C), can be observed. After treating the graphite via the modified Hummer method, new peaks of 1050 and 1720 cm^{-1} emerged. These peaks can be ascribed to the presence of C-O and C=O bonds, respectively. The above change was accompanied by a stronger intensity of the absorption band at 3400 cm^{-1}, which represents the hydroxyl groups. These spectral changes indicate the presence of carbonyl, ether, and hydroxyl groups in the chemical structure of the treated graphite, implying that graphene oxide has been produced. After treating the graphene oxide with vitamin C, the intensity of OH band (3400 cm^{-1}) and C=O (1720 cm^{-1}) and C-O (1050 cm^{-1}) peaks decreased. The above spectral changes suggest that the graphene oxide was reduced.

The reduction of graphene oxide by vitamin C was also confirmed by considering the Raman spectra of graphene oxide (GO) both before and after treating it with vitamin C (Figure 2). Here, the characteristic D band and G band, representing sp^3 hybridization and sp^2 hybridization of the graphene oxides (both before and after reduction), can be observed at 1344–1364 cm^{-1} and 1573–1603 cm^{-1}, respectively. Consideration of the D/G band intensity ratios (designated as I_D/I_G in Table 1) reveals that the I_D/I_G value increased after the reduction of GO. A similar effect was observed by Chen and Yan [12]. This change can be attributed to the decrease in the average size of the in-plane sp^2 domains, through the reduction process of GO. After heat treatment,

Table 1: Intensity ratios of the Raman bands (I_D/I_G) and percentage mass of elements from EDX techniques of graphite, graphene oxide (GO), and reduced graphene oxide (rGO).

Samples	Before heat treatment			After heat treatment		
	Raman bands	Percentage mass from EDX		Raman bands	Percentage mass from EDX	
	I_D/I_G	C	O	I_D/I_G	C	O
Graphite	0.257	N/A	N/A	N/A	N/A	N/A
GO	0.802	52.55	47.44	0.960	52.58	47.40
rGO	0.975	71.04	28.95	1.002	64.11, 15.98	35.89, 84.02

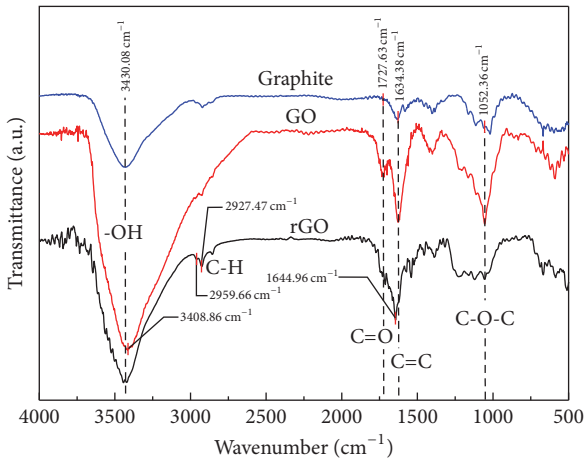

Figure 1: FTIR spectra of graphite, graphene oxide (GO), and reduced graphene oxide (rGO).

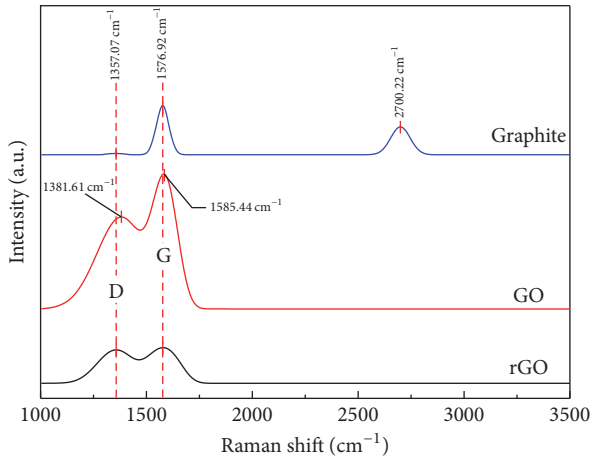

Figure 2: Raman spectra of graphite, graphene oxide, and reduced graphene oxide.

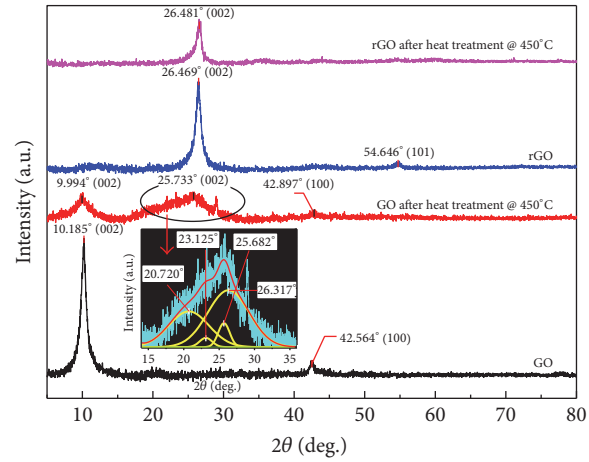

Figure 3: XRD patterns of GO and rGO, both before and after heat treatment.

the Raman spectra of both GO and rGO still exist. The I_D/I_G value of GO increased after the heat treatment. It was apparent that the hybridization of GO had been transformed during the heat treatment process. The above effect was not the case for heat treated rGO.

The formation of reduced graphene oxide, via either chemical reaction with vitamin C or thermal reduction, can also be followed up by considering the XRD patterns of various graphene based materials (Figure 3). After experiencing the chemical reduction, the characteristic peaks at $2\theta = 10.1^\circ$, representing graphene oxide, shifted to $2\theta = 26.33^\circ$ and 53.45°. The positions of these peaks correspond to those of the neat graphite. Similarly, after the heat treatment process, the XRD pattern of graphene oxide significantly changed. The intensity of the peak at $2\theta = 10.1^\circ$ decreased whereas a new peak at 26.31° emerged. Again, the positions of these peaks are close to those of the neat graphite and the reduced graphene oxide, respectively. These indicate that the graphene oxide was partly reduced through the heat treatment process.

Figure 4 shows the SEM images of graphene oxide and reduced graphene oxide. The presence of two-dimensional wrinkled sheets measuring the length of several micrometers can be noted from the SEM images of both GO and rGO. After the heat treatment, the characteristic wrinkled sheets of GO were still retained. This was also the case for rGO that experienced the same heat treatment process. Attempts were also made to characterize GO and rGO specimens by using an EDX technique. From the quantitative analysis, the amounts of oxygen (O) and carbon (C) elements were determined and are summarized in Table 1. The percentage mass of the oxygen atom significantly decreased from 47.44% to 28.95% after treating the GO with the reducing agent (vitamin C). This can be considered as indirect evidence supporting the formation of rGO. Based on the above results from FTIR, Raman spectra, XRD, SEM, and EDX, it can be concluded that the GO and rGO were successfully prepared.

3.2. Effects of GO and rGO on Structures and Properties of TiO_2. Figure 5 shows the overlaid XRD patterns of TiO_2

Table 2: Crystal size and bandgap energy values of TiO_2 and graphene/TiO_2 composites.

Sample codes	Type & content of graphene		Crystallite size (nm)[#]	Bandgap energy (eV)
	GO (wt%)	rGO (wt%)		
TiO_2	—	—	19.27	3.03
Ti@GO-01	0.01	—	19.47	2.98
Ti@GO-03	0.03	—	19.61	2.97
Ti@GO-05	0.05	—	19.81	2.98
Ti@GO-10	0.10	—	19.01	2.99
Ti@rGO-01	—	0.01	18.28	2.95
Ti@rGO-03	—	0.03	19.25	2.98
Ti@rGO-05	—	0.05	19.45	3.00
Ti@rGO-10	—	0.10	19.56	3.02

[#]The average crystal size estimated from XRD line-broadening of the TiO_2 (101) diffraction peaks.

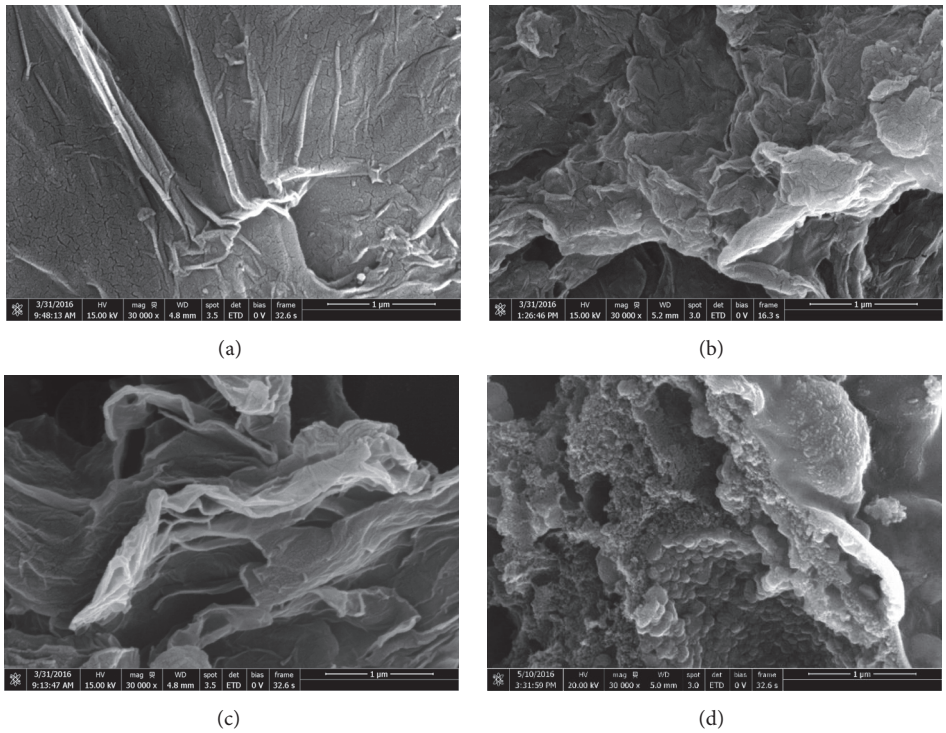

Figure 4: SEM micrographs of GO (a) and rGO (b); the heat treated GO (c); and the heat treated rGO (d).

and various graphene/TiO_2 composites. The diffraction peaks representing anatase and rutile phases TiO_2 can be assigned in accordance with JCPDS cards numbers 21-1272 and 21-1276. After mixing TiO_2 with graphene, the characteristic peaks of TiO_2 still exist. Attempts were also made to determine the average crystal size of TiO_2 by using the Scherrer equation. The results, illustrated in Table 2, show that the crystal size of TiO_2 did not change significantly with the presence of either GO or rGO. It seems that the characteristic peaks of GO and rGO were obscured by those of TiO_2, which is the majority of the composite materials. In this regard, a change in XRD patterns of graphene/TiO_2 upon heat treatment should not be expected.

Consideration of SEM images of the composites (Figure 6) reveals that the porous structure consisting of interconnected particulate structure of the titania was retained. The above results indicate that the presence of graphene (either GO or rGO) did not affect the morphology and microstructure of the titania. Again, this can be ascribed to the fact that the amount of GO and rGO used for modifying TiO_2 was relatively low compared to that of the neat titania. Figure 7 shows the cross-sectional SEM image of the TiO_2 based photoelectrode. The porous structure of the mesoscopic layer, made from GO/TiO_2, can be observed. This layer was perfectly laid on top of the TiO_x coated FTO. The thickness values of each layer were approximately 5 μm,

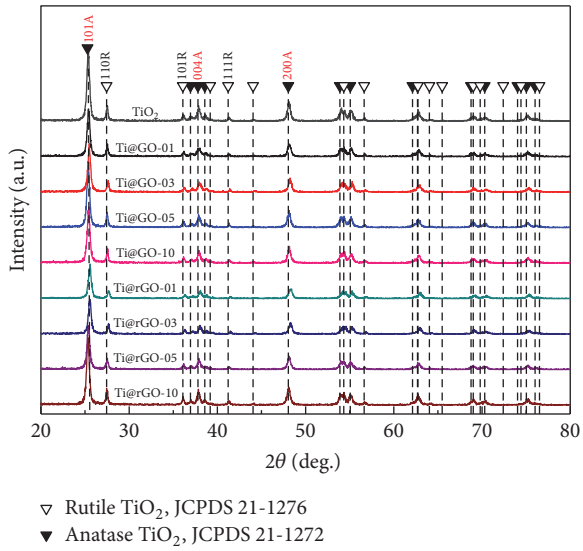

Figure 5: XRD patterns of TiO_2 and the various graphene/TiO_2 composites.

300 nm, and 600 nm, respectively. These ranges were found to be reasonable and in agreement with that which was reported in related references [20, 21].

Figure 8 shows typical UV-Vis spectra of the various solid graphene/TiO_2 composites. As a result, the bandgap energy values of various samples were determined and are summarized in Table 2. The calculated bandgap energy of the neat TiO_2 was 3.03 eV, which is similar to that which has been reported in the literature [22]. After applying GO to TiO_2, the bandgap energy values of the composites only slightly decreased to the range of 2.97–2.99 eV. The values did not change significantly with the concentration of GO, probably due to the fact that the amount of GO used for modifying TiO_2 was marginal. Therefore, the interaction between TiO_2 and GO was not different, regardless of the GO concentration. A similar effect was observed when rGO was applied to TiO_2. In this latter case, the bandgap energy values of rGO/TiO_2 ranged between 2.95 and 3.02 eV. Figure 9 shows XPS spectra of various graphene and graphene/TiO_2 composite materials. After deconvolution, 5 different peaks can be designated. These are those representing sp^2 of C=C/C-C (of the basal plane) at 284.97 eV, C-OH (of the hydroxyl group) at 285.88 eV, C-O-C (of the epoxide group) at 286.86 eV, >C=O (of the carbonyl group) at 287.84 eV, and C(O)OH (of the carboxyl group) at 288.94 eV. From the above results, it can be seen that intensity of the peaks representing the carbonyl and the epoxide groups decreased after thermal reduction. Intensity of the peaks representing carbon-carbon bonds in the annealed GO (Figure 9(b)) is also greater than those of the annealed rGO (Figure 9(d)). This suggests that electrical properties of the former should be better than of the latter. The above results also imply that the thermal reduction method is more effective than the chemical reduction approach, taking into account the relative intensity of the C-C peaks from the two systems. For the composite materials, it is also noteworthy that the intensity of the peaks relating to the carboxylic group of Ti@rGO-01 (Figure 9(e)) increased after annealing. This suggests that TiO_2 might induce the oxidation of rGO phase in the composite during heat treatment.

By using the above bandgap energy values in combination with the energy levels of each electrode system, which was determined from the XPS technique, the energy band diagrams of the DSSCs can be evaluated and are illustrated in Figure 10. The diagram mentioned in Figure 10 reveals that the valence band (VB), the conduction band (CB), and the bandgap energy values of Ti@GO are 2.33, −0.65, and 2.98 eV, respectively. The energy levels of CB and VB of the composite electrode also lied between those of the adjacent layers (the FTO and the adsorbed dye), implying the efficient transportation of electrons and holes in the system.

In terms of light harvesting properties, considerations of the UV-visible spectra of various materials in the liquid suspension state (Figure 11) revealed that the neat GO is also capable of absorbing light in a wide wavelength, ranging from 200 nm to 600 nm. Notably, this absorption range is also overlapping with the light absorption of the dye. The intensity from the absorption peaks of graphene/TiO_2 composites is also greater than that of the neat TiO_2. The absorption intensity of TiO_2 initially increased with the concentration of GO, to the maximum value at 0.10 wt% GO loading. At a higher concentration of GO (0.15 wt%), however, the intensity dropped again. This was probably due to some agglomeration of the graphene oxide. Similarly, rGO was capable of absorbing light in a wavelength ranging from 210 to 350 nm. The absorbance of rGO/TiO_2 composites was also greater than that of the neat TiO_2. The absorbance of rGO/TiO_2 composites seems to be slightly inferior to those of the GO/TiO_2 system. Nevertheless, the above results imply that the absorbance of the dye, which is the actual light harvester for the DSSC system, could be interfered with or suppressed by the graphene/TiO_2 electrode. The above phenomenon might affect the power conversion efficiency of the cells.

3.3. Photovoltaic Performance of the GO/TiO_2 Based DSSCs. Figure 12 shows typical *I-V* curves of the various DSSCs, resulting in photovoltaic parameters that are determined and summarized in Table 3. It can be seen that the V_{oc} values of the cells hardly changed with the concentration of GO used for modifying the TiO_2 photoelectrode. This suggests that the addition of graphene did not affect the Fermi level of TiO_2 [1, 13, 14]. However, the short-circuit current density (J_{sc}) and the power conversion efficiency (PCE) values of the GO/TiO_2 based cells are greater than those of the normal cell (without graphene). The PCE value of the cell initially increased when 0.01 wt% of GO was applied to the TiO_2 electrode. After that, the PCE value of the cells decreased again with the increase of the concentration of GO in the composite electrode. In our opinion, it seems that the effects of GO on the photovoltaic performance of the DSSC based on the TiO_2 electrode were not straightforward, depending on the concentration of the graphene oxide. In fact, a similar trend was noted by Kusumawati et al. [14] and Wang et al. [13] whereby the relationship between the concentration of graphene and PCE and J_{sc} of the cell was nonlinear and

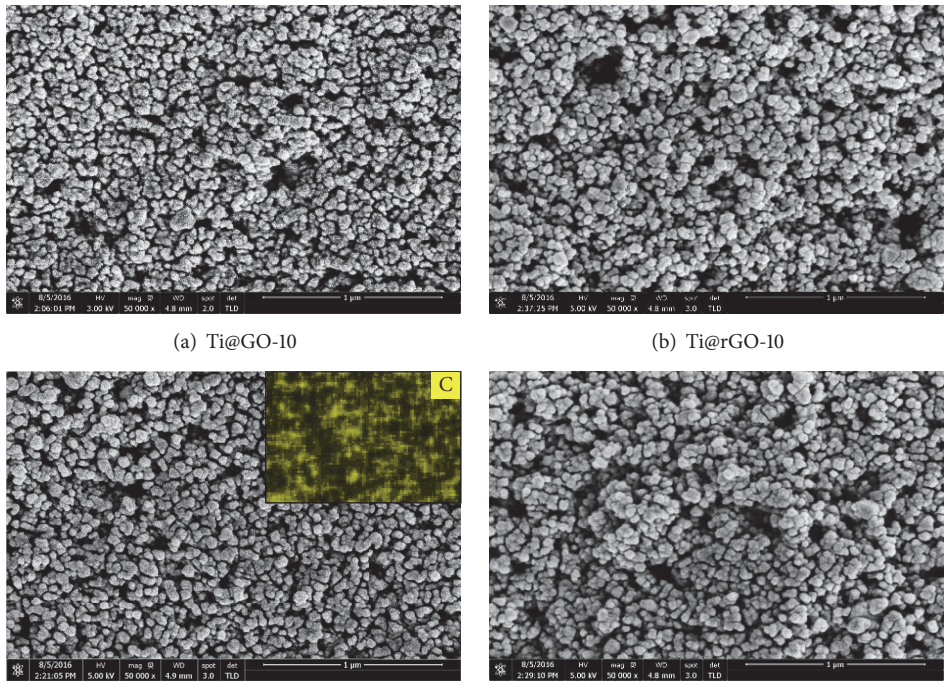

(a) Ti@GO-10 (b) Ti@rGO-10

(c) Ti@GO-10 (after heat treatment) (d) Ti@rGO-10 (after heat treatment)

FIGURE 6: SEM images of GO/TiO_2 and rGO/TiO_2 composites, before and after heat treatment (inset images are EDS mapping of carbon element).

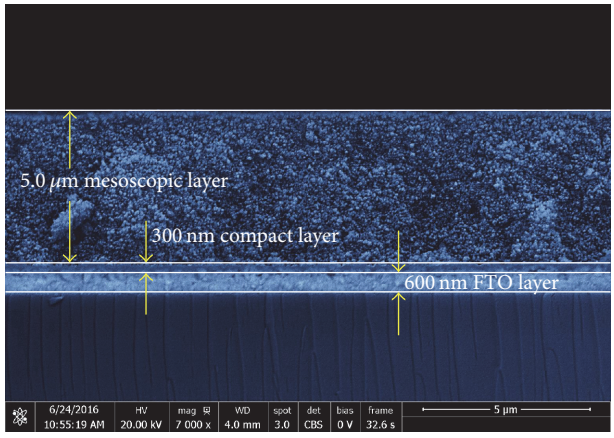

FIGURE 7: SEM image of the cross section of the DSSC photoanode comprised of FTO, compact layer, and the TiO_2 based mesoscopic layer (Ti@GO-01).

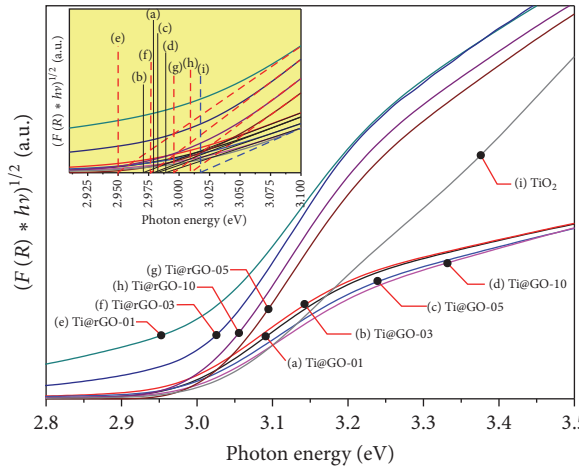

FIGURE 8: UV-Vis spectra of the various solid graphene/TiO_2 composites.

exhibited a kind of volcano shape. In this regard, it was believed that the presence of GO in the DSSC system not only affected the performance of the TiO_2 electrode, but also influenced the performance of other components in the cell. It was also possible that these effects were competing. Generally, the promoting effects of reduced graphene oxides on the DSSC performance of TiO_2 have been attributed to several mechanisms. These include (i) the increase of dye loading due to the higher surface area of the graphene modified photoelectrode and (ii) the decrease of electron-hole recombination due to the enhancement of electron transfer from TiO_2 to the photoelectrode. For example, work by Wang et al. [13] showed that the percentage of the dye loading of graphene/TiO_2 electrodes did not change with the GO content, and the promoting effect of GO on the DSSC performance of TiO_2 was attributed to the greater electron transfer. On the other hand, Kusumawati et al. [14] reported that, by using GO/TiO_2 as a replacement of TiO_2, the charge transfer of the system did not change, regardless of the GO content. In that case, the better performance of the DSSC based on the GO/TiO_2 electrode resulted in a higher amount of dye loading in the cell.

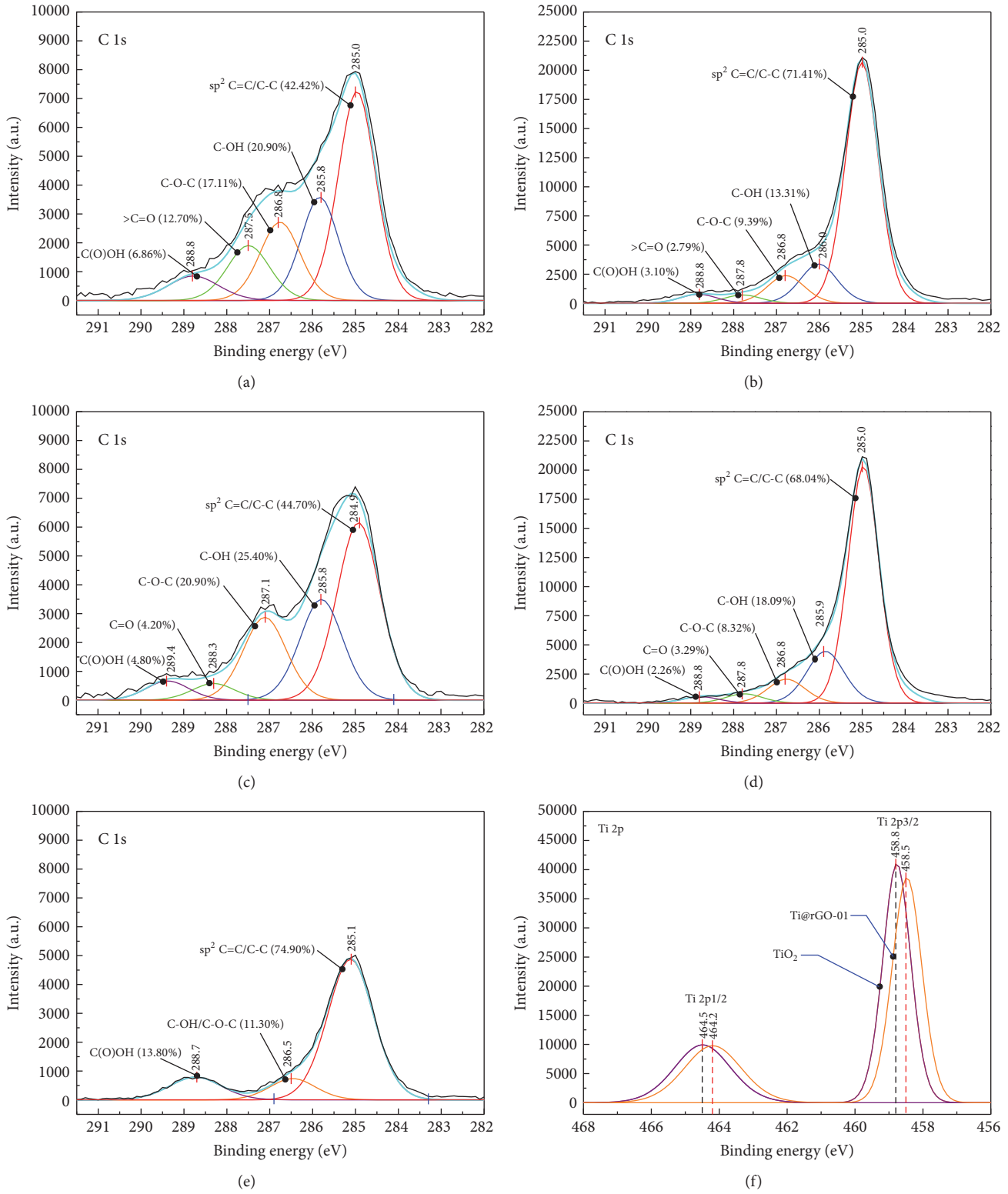

Figure 9: XPS spectra of various graphene based materials: (a) C 1s of GO (before heat treatment); (b) C 1s of GO (after heat treatment); (c) C 1s of rGO (before heat treatment); (d) C 1s of rGO (after heat treatment); (e) C 1s of Ti@rGO-01; (f) Ti 2p of Ti@rGO-01.

Table 3: Short-circuit current density (J_{sc}), open-circuit voltage (V_{oc}), fill factor (FF), power conversion efficiency (PCE), charge recombination resistance (R_{rec}), and electron lifetime (τ_e) of the DSSCs containing various types and amounts of graphene.

Sample codes	J_{sc} (mA/cm^2)	V_{oc} (V)	FF	PCE (%)	R_{2rec} (Ω)	τ_e (μsec)
TiO_2	6.27	0.71	60.28	2.68	14.07	79.74
Ti@GO-01	8.42	0.68	63.99	3.69	26.74	226.81
Ti@GO-03	7.51	0.68	62.98	3.22	20.94	150.22
Ti@GO-05	7.14	0.69	64.7	3.2	19.18	119.46
Ti@GO-10	6.22	0.7	66.83	2.92	16.09	105.21
Ti@rGO-01	2.79	0.63	72.23	1.28	5.79	26.51
Ti@rGO-03	6.31	0.7	65.29	2.9	16.08	92.83
Ti@rGO-05	5.52	0.63	64.11	2.38	10.51	54.99
Ti@rGO-10	5.38	0.63	65.56	2.32	9.08	42.81

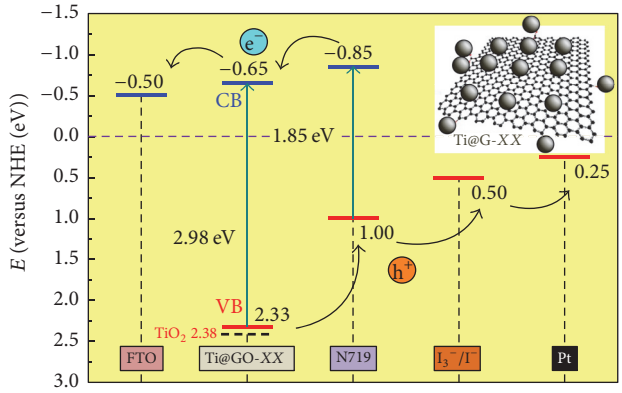

Figure 10: Band diagram of DSSC containing graphene/TiO_2 electrode.

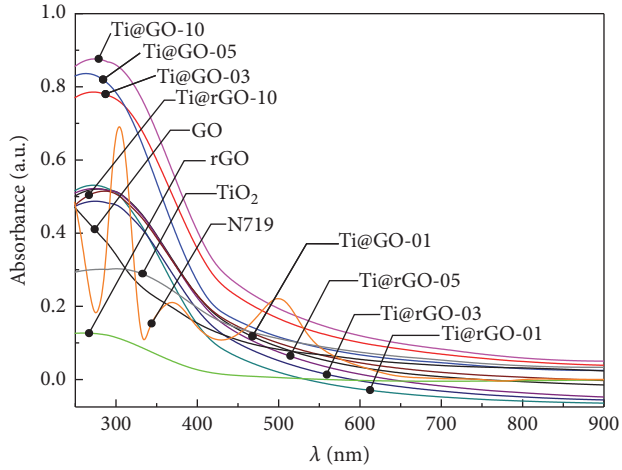

Figure 11: UV-Vis spectra of TiO_2, GO, rGO, and the various graphene/TiO_2 electrodes.

In this study, we found that the percentage of dye loading of the TiO_2 based electrodes did not increase after applying GO into the TiO_2 electrode (Figure 13). Therefore, the greater PCE of the cells containing graphene could be attributed to some other factors. Figures 14 and 15 show EIS spectra and Bode imaginary plots of various DSSCs. In addition, the equivalent circuit, representing the cell reaction under the backward condition, was also illustrated. Generally, the term R_1 refers to ohmic series resistance, describing the contact between FTO/TiO_2 interfaces. The parameter Z_{W2} denotes charge diffusion impedance of the electron in TiO_2 electrode whereas R_2 refers to charge recombination resistance (R_{rct}) of the TiO_2 based electrode. In this study, it was found that R_1 did not change with the type and concentration of the graphene used. However, R_{rct} value of the cells increased after applying GO into the TiO_2 electrode. Lifetime of the electron (τ_e) in the GO/TiO_2 based DSSCs was also longer than that of the normal DSSC based on the neat TiO_2 electrode. The above results suggest that the electron-hole recombination in the system could be suppressed and that contributed to the greater efficiency of the DSSCs. In addition, a consideration of the energy band diagrams (Figure 10) of the graphene/TiO_2 based DSSCs suggested that transportation of electron and hole from the excited dye toward the corresponding electrode could be facilitated with the presence of the graphene/TiO_2 electrode. The above effect could be related to the better PCE of the cell.

It is noteworthy, as mentioned above, that the relationship between GO content and the PCE values of the cells was nonlinear. The efficiency values decreased as the concentration of GO was further increased above 0.01 wt%. In our opinion, this could be related to other effects, including the lower light harvesting property of the dye, which was suppressed by the absorption of light by GO in a similar wavelength range (200–800 nm) (Figure 11). Consequently, the number of photogenerated electrons was reduced and that contributed to the decrease in PCE values of the DSSCs at the high concentration of GO. This effect is similar to that which was observed by Wang et al. [13].

3.4. Photovoltaic Performance of the rGO/TiO_2 Based DSSCs. When rGO was used as a replacement of GO in the composites electrode, a similar trend was observed, except that the optimum concentration of rGO yielding the highest PCE value of DSSC had shifted to 0.03 wt%. Beyond this concentration, the PCE values of the system decreased again. The relationship between rGO content and various parameters, such as J_{sc}, R_{rec}, and τ_e, also followed that same trend. By applying more than 0.03 wt% of rGO, the V_{oc} value significantly dropped. This indicates that the Fermi level of the TiO_2 electrode was affected by the presence of rGO. In this case,

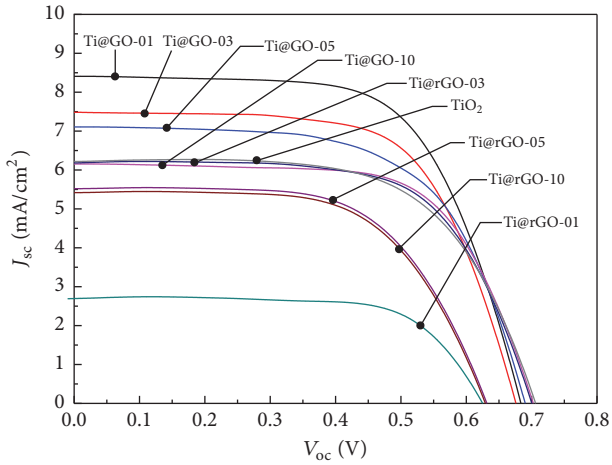

FIGURE 12: J-V curves of DSSCs containing different types of TiO_2 based electrodes.

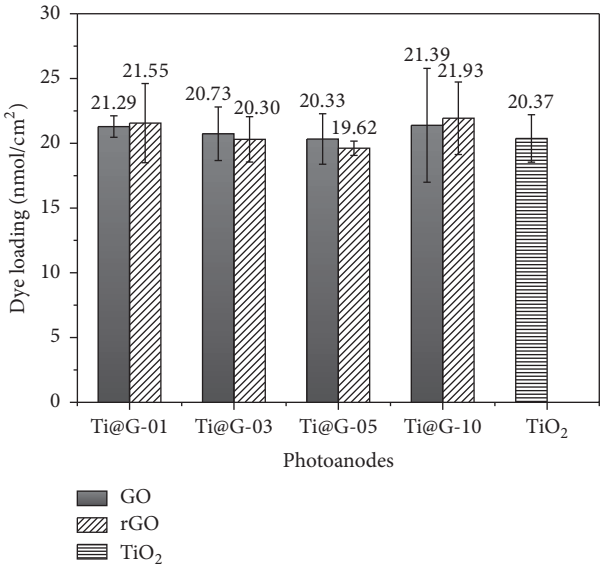

FIGURE 13: Dye loading contents of various TiO_2 based electrodes.

this was probably because some electron-hole recombination at the interface between graphene and liquid electrolyte occurred and contributed to the lower V_{oc} values and the shift of the Fermi level of the rGO/TiO_2 composite electrode.

It is also worth noting that the PCE values of many DSSCs based on rGO/TiO_2 electrodes were lower than those of the GO/TiO_2 based DSSCs, provided that the same concentration of graphene was used (0.01–0.05 wt%). In our opinion, the above discrepancy can be related to several factors, including the differences in light absorption properties and charge transportation of the two electrode systems. For example, the above results from EIS technique (Figures 14 and 15) show that charge recombination resistance and electron lifetime of the GO/TiO_2 based DSSCS are greater than those of the rGO/TiO_2 based cells. Raman spectra of the composite electrodes (Figure 16) also showed that the characteristic D and G bands of the reduced graphene oxide in the composite (Ti@rGO-05) disappeared after the heat treatment process.

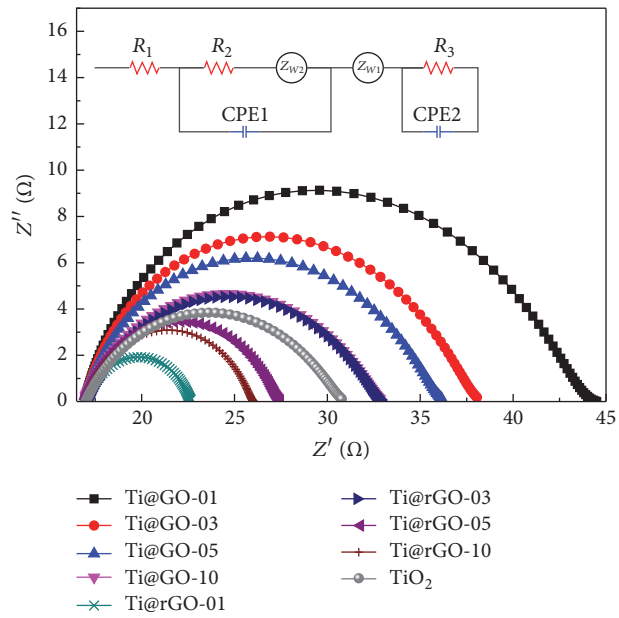

FIGURE 14: EIS spectra of various TiO_2 and graphene/TiO_2 based DSSCs.

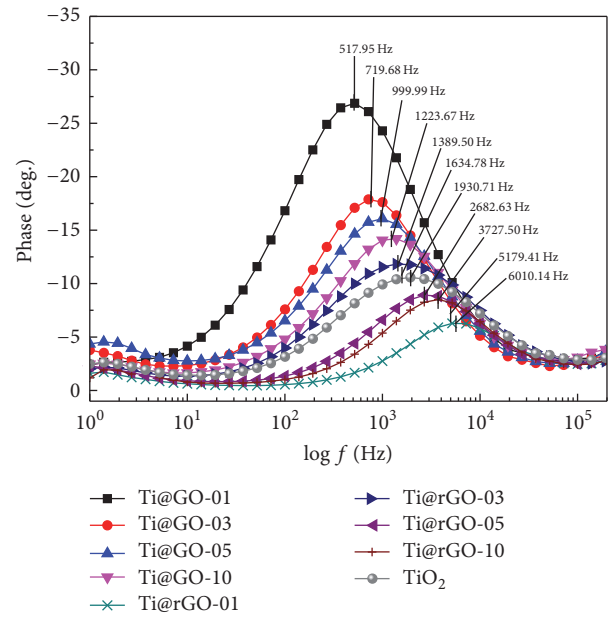

FIGURE 15: Bode imaginary plots for the impedance of DSSCs containing different types of TiO_2 based photoanodes.

This was not the case of the GO/TiO_2 composite (Ti@GO-05). It is apparent that the rGO phase in the TiO_2/rGO composite was partially degraded during the heat treatment process. In our opinion, it was believed that the presence of TiO_2 in the composite had induced the degradation of the rGO via some possible mechanisms such as scission and oxidation of the graphene plane. This resulted in the formation of oxidized functional groups such as carboxylic acid on the edge [23]. The above notion was supported by the result from XPS technique in which the C 1s peak at 288.74 eV emerged (Figure 9(e)).

Table 4: Comparative DSSC performance of the various graphene/TiO_2 electrodes from different works.

References	Photoanode materials	Cell descriptions		PCE (%) of cells with different electrodes	
		Optimum graphene content (wt%)	Active area (cm^2)	Graphene/TiO_2	Bare TiO_2
Wang et al., 2012	GO/TiO_2	0.83	0.50	2.78	1.79
Kusumawati et al., 2014	GO/TiO_2	1.20	0.36	7.49	5.78
Cheng and Stadler, 2015	GO/TiO_2	1.60	0.25	7.68	4.78
Chou et al., 2015	GO/TiO_2	0.05	0.57	5.26	n/a
Ding et al., 2015	rGO/TiO2	0.75	n/a	7.89	6.06
Tang et al., 2010	rGO/TiO_2	10.0*	0.25	1.68	0.32
This study	rGO/TiO_2	0.03	0.40	2.90	2.68
This study	rGO/TiO_2	0.01	0.40	1.28	2.68
This study	GO/TiO_2	0.01	0.40	3.69	2.68

∗ refers to %w/v of RGO as compared to titanium(IV) butoxide colloids.

Last but not least, for comparative purposes, the best PCE values of DSSCs based on graphene/TiO_2 electrodes from this study and those reported in some additional literature are summarized in Table 4. It is noteworthy that the PCE values of DSSCs obtained from this study are in a reasonable range, even though some discrepancies can be seen. In our opinion, these differences can be attributed to several factors including the graphene content, the actual thickness of each layer in the devices, and the active area of the cells. Nevertheless, overall, our results demonstrate that a small amount of graphene oxide (0.01–0.05 wt%), which was thermally reduced in situ during the fabrication process of DSSC, can be used to promote the photovoltaic performance of the TiO_2 electrode. In this regard, the photovoltaic performance of the graphene/TiO_2 electrodes in the perovskite solar cell also deserves consideration and in fact is an aspect included in our ongoing work.

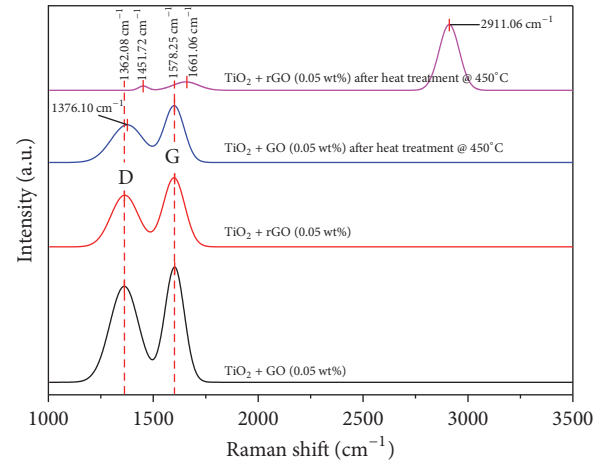

Figure 16: Raman spectra of graphene/TiO_2 composites both before and after heat treatment.

4. Conclusions

(1) Two different types of graphene based materials were successfully prepared by using two different approaches:

(i) The reduced graphene oxide which was pretreated with a mild reducing agent (vitamin C) prior to use (the so-called rGO herein).

(ii) The graphene oxide which could be thermally reduced in situ (the so-called GO) during the annealing step of the solar cell fabrication process.

(2) The prepared graphene was capable of harvesting light in the wavelength which overlapped with that of the dye. The light absorption intensity of the TiO_2 based composites also increased with the graphene concentration. These factors contributed to the lowering of the power conversion efficiency of the TiO_2 based DSSCs.

(3) The relationships between the concentration of (r)GO in the graphene/TiO_2 based photoanodes and the power conversion efficiency (PCE) of the DSSCs were nonlinear. The PCE initially increased in the presence of 0.01 wt% of GO. As the GO was further increased, the PCE value decreased. Similar effects were observed when rGO was used as a dopant.

(4) Regardless of the graphene types, the promoting effect of graphene on the photovoltaic performance of TiO_2 was related to the greater resistance to electron-hole recombination and a longer electron lifetime. On the other hand, the decreasing trends of PCE and J_{sc} values of DSSCs of high graphene (GO and/or rGO) content can be ascribed to the competing light harvesting efficiency between the dye and the graphene.

(5) In this study, the maximum power conversion efficiency value of DSSC (3.69%, FF = 63.98, V_{oc} = 0.68, and I_{sc} = 8.42) was obtained when only a small amount (0.01 wt%) of the thermally reduced GO was added to the TiO_2 based photoelectrode. This corresponded to an improvement of 73%, compared to that of the DSSC employing the bare TiO_2 electrode (2.13%, FF = 65.07, V_{oc} = 0.68, and I_{sc} = 4.75).

Conflicts of Interest

The authors declare that there are no conflicts of interest regarding the publication of this paper.

Acknowledgments

This work has been supported by the Nanotechnology Center (Nanotec), NSTDA, Ministry of Science and Technology, Thailand, through its programme of the Center of Excellence Network.

References

[1] http://www.nrel.gov/ncpv/images/efficiency_chart.jpg.

[2] H. Ding, S. Zhang, J.-T. Chen et al., "Reduction of graphene oxide at room temperature with vitamin C for RGO–TiO_2 photoanodes in dye-sensitized solar cell," *Thin Solid Films*, vol. 584, pp. 29–36, 2015.

[3] Y.-B. Tang, C.-S. Lee, J. Xu et al., "Incorporation of graphenes in nanostructured TiO_2 films via molecular grafting for dye-sensitized solar cell application," *ACS Nano*, vol. 4, no. 6, pp. 3482–3488, 2010.

[4] G. S. Han, Y. H. Song, Y. U. Jin et al., "Reduced graphene oxide/mesoporous TiO_2 nanocomposite based perovskite solar cells," *ACS Applied Materials and Interfaces*, vol. 7, no. 42, pp. 23521–23526, 2015.

[5] S. Park, J. An, I. Jung et al., "Colloidal suspensions of highly reduced graphene oxide in a wide variety of organic solvents," *Nano Letters*, vol. 9, no. 4, pp. 1593–1597, 2009.

[6] A. K. Swain and D. Bahadur, "Enhanced stability of reduced graphene oxide colloid using cross-linking polymers," *Journal of Physical Chemistry C*, vol. 118, no. 18, pp. 9450–9457, 2014.

[7] M. J. Fernández-Merino, L. Guardia, J. I. Paredes et al., "Vitamin C is an ideal substitute for hydrazine in the reduction of graphene oxide suspensions," *Journal of Physical Chemistry C*, vol. 114, no. 14, pp. 6426–6432, 2010.

[8] J. Zhang, H. Yang, G. Shen, P. Cheng, J. Zhang, and S. Guo, "Reduction of graphene oxide via L-ascorbic acid," *Chemical Communications*, vol. 46, no. 7, pp. 1112–1114, 2010.

[9] Y. Matsumoto, M. Koinuma, S. Y. Kim et al., "Simple photoreduction of graphene oxide nanosheet under mild conditions," *ACS Applied Materials and Interfaces*, vol. 2, no. 12, pp. 3461–3466, 2010.

[10] A. Hasani, H. Sharifi Dehsari, A. Amiri Zarandi, A. Salehi, F. A. Taromi, and H. Kazeroni, "Visible light-assisted photoreduction of graphene oxide using CdS nanoparticles and gas sensing properties," *Journal of Nanomaterials*, vol. 2015, Article ID 930306, 11 pages, 2015.

[11] H. Tong, J. Zhu, J. Chen et al., "Electrochemical reduction of graphene oxide and its electrochemical capacitive performance," *Journal of Solid State Electrochemistry*, vol. 17, no. 11, pp. 2857–2863, 2013.

[12] W. Chen and L. Yan, "Preparation of graphene by a low-temperature thermal reduction at atmosphere pressure," *Nanoscale*, vol. 2, no. 4, pp. 559–563, 2010.

[13] H. Wang, S. L. Leonard, and Y. H. Hu, "Promoting effect of graphene on dye-sensitized solar cells," *Industrial and Engineering Chemistry Research*, vol. 51, no. 32, pp. 10613–10620, 2012.

[14] Y. Kusumawati, M. A. Martoprawiro, and T. Pauporté, "Effects of graphene in graphene/TiO_2 composite films applied to solar cell photoelectrode," *Journal of Physical Chemistry C*, vol. 118, no. 19, pp. 9974–9981, 2014.

[15] G. Cheng and F. J. Stadler, "Achieving phase transformation and structure control of crystalline anatase TiO_2@C hybrids from titanium glycolate precursor and glucose molecules," *Journal of Colloid and Interface Science*, vol. 438, pp. 169–178, 2015.

[16] J.-C. Chou, C.-H. Huang, Y.-H. Liao, S.-W. Chuang, L.-H. Tai, and Y.-H. Nien, "Effect of different graphene oxide contents on dye-sensitized solar cells," *IEEE Journal of Photovoltaics*, vol. 5, no. 4, pp. 1106–1112, 2015.

[17] W. Shu, Y. Liu, Z. Peng, K. Chen, C. Zhang, and W. Chen, "Synthesis and photovoltaic performance of reduced graphene oxide-TiO_2 nanoparticles composites by solvothermal method," *Journal of Alloys and Compounds*, vol. 563, pp. 229–233, 2013.

[18] O. O. Kapitanova, G. N. Panin, A. N. Baranov, and T. W. Kang, "Synthesis and properties of graphene oxide/graphene nanostructures," *Journal of the Korean Physical Society*, vol. 60, no. 10, pp. 1789–1793, 2012.

[19] W. S. Hummers Jr. and R. E. Offeman, "Preparation of graphitic oxide," *Journal of the American Chemical Society*, vol. 80, no. 6, p. 1339, 1958.

[20] L. Meng and C. Li, "Blocking layer effect on dye-sensitized solar cells assembled with TiO_2 nanorods prepared by dc reactive magnetron sputtering," *Nanoscience and Nanotechnology Letters*, vol. 3, no. 2, pp. 181–185, 2011.

[21] Y. Zheng, S. Klankowski, Y. Yang, and J. Li, "Preparation and characterization of TiO_2 barrier layers for dye-sensitized solar cells," *ACS Applied Materials and Interfaces*, vol. 6, no. 13, pp. 10679–10686, 2014.

[22] S. Valencia, J. M. Marín, and G. Restrepo, "Study of the bandgap of synthesized titanium dioxide nanoparticules using the sol-gel method and a hydrothermal treatment," *Open Materials Science Journal*, vol. 4, pp. 9–14, 2009.

[23] M. Xing, W. Fang, X. Yang, B. Tian, and J. Zhang, "Highly-dispersed boron-doped graphene nanoribbons with enhanced conductibility and photocatalysis," *Chemical Communications*, vol. 50, no. 50, pp. 6637–6640, 2014.